

RL-TR-96-241
Final Technical Report
February 1997



OPTICAL IMAGE CORRELATION USING WAVELENGTH MULTIPLEXED VOLUME HOLOGRAMS

Accuwave Corporation

Koichi Sayano and Feng Zhao

APPROVED FOR PUBLIC RELEASE; DISTRIBUTION UNLIMITED.

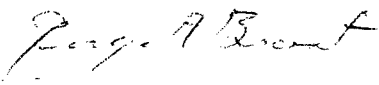
19970416 005


DTIC QUALITY INSPECTED 4

**Rome Laboratory
Air Force Materiel Command
Rome, New York**

This report has been reviewed by the Rome Laboratory Public Affairs Office (PA) and is releasable to the National Technical Information Service (NTIS). At NTIS it will be releasable to the general public, including foreign nations.

RL-TR-96-241 has been reviewed and is approved for publication.

APPROVED: 
GEORGE A. BROST
Project Engineer


FOR THE COMMANDER:
FRED J. DEMMA, Acting Director
Surveillance & Photonics Directorate

If your address has changed or if you wish to be removed from the Rome Laboratory mailing list, or if the addressee is no longer employed by your organization, please notify RL/OCPA, 25 Electronic Pky, Rome, NY 13441-4514. This will assist us in maintaining a current mailing list.

Do not return copies of this report unless contractual obligations or notices on a specific document require that it be returned.

REPORT DOCUMENTATION PAGE			Form Approved OMB No. 0704-0188	
Public reporting burden for this collection of information is estimated to average 1 hour per response, including the time for reviewing instructions, searching existing data sources, gathering and maintaining the data needed, and completing and reviewing the collection of information. Send comments regarding this burden estimate or any other aspect of this collection of information, including suggestions for reducing this burden, to Washington Headquarters Services, Directorate for Information Operations and Reports, 1215 Jefferson Davis Highway, Suite 1204, Arlington, VA 22202-4302, and to the Office of Management and Budget, Paperwork Reduction Project (0704-0188), Washington, DC 20503.				
1. AGENCY USE ONLY (Leave blank)		2. REPORT DATE February 1997		3. REPORT TYPE AND DATES COVERED FINAL, Jun 95 - Jun 96
4. TITLE AND SUBTITLE OPTICAL IMAGE CORRELATION USING WAVELENGTH MULTIPLEXED VOLUME HOLOGRAMS			5. FUNDING NUMBERS C - F30602-95-C-0150 PE - 62702F PR - 4600 TA - P4 WU - PW	
6. AUTHOR(S) Koichi Sayano, Feng Zhao				
7. PERFORMING ORGANIZATION NAME(S) AND ADDRESS(ES) Accuwave Corporation 1651 19th St. Santa Monica CA 90404			8. PERFORMING ORGANIZATION REPORT NUMBER	
9. SPONSORING / MONITORING AGENCY NAME(S) AND ADDRESS(ES) Rome Laboratory/OCPA 25 Electronic Pky Rome NY 13441-4515			10. SPONSORING / MONITORING AGENCY REPORT NUMBER RL-TR-96-241	
11. SUPPLEMENTARY NOTES Rome Laboratory Project Engineer: George Brost, OCPA, (315) 330-7669				
12a. DISTRIBUTION AVAILABILITY STATEMENT Approved for public release; distribution unlimited.			12b. DISTRIBUTION CODE	
13. ABSTRACT (Maximum 200 words) An optical image correlator using a spatial light modulator (SLM) for reference image recording and correlation readout has been demonstrated. The reference image correlation filters are recorded in a volume holographic optical element using wavelength multiplexing. Auto- and cross-correlations between similar and dis-similar images were compared to determine the image discrimination characteristics of the optical correlator.				
14. SUBJECT TERMS optical correlator, pattern recognition, volume holography, Fourier optics			15. NUMBER OF PAGES 28	
			16. PRICE CODE	
17. SECURITY CLASSIFICATION OF REPORT UNCLASSIFIED	18. SECURITY CLASSIFICATION OF THIS PAGE UNCLASSIFIED	19. SECURITY CLASSIFICATION OF ABSTRACT UNCLASSIFIED	20. LIMITATION OF ABSTRACT UNLIMITED	

OPTICAL IMAGE CORRELATION USING WAVELENGTH MULTIPLEXED VOLUME HOLOGRAMS

FINAL TECHNICAL REPORT

INTRODUCTION

Accuwave Corporation has demonstrated an optical image correlator using a compact spatial light modulator (SLM) for both reference image input during recording and loading the unknown test image during operation. The SLM replaces the chrome on glass image-bearing transparencies that had been used as test images in past optical image correlation experiments. Issues affecting discrimination of auto- vs. cross-correlation outputs such as dc suppression, edge enhancement, and thresholding methods have also been addressed in this program.

Optical processing provides significant speed advantages in many pattern recognition applications, particularly those requiring comparison against a large number of complex reference images. The correlation operation is one such function that can be implemented optically in conjunction with holographic storage to take advantage of its parallel architecture for fast readout. Fourier transforms and inverse transforms are generated optically, and the reference image Fourier transforms are recorded in a volume holographic, wavelength-multiplexed element. An unknown input image is then compared to all of the stored images using the optically generated correlation. This approach provides considerable processing speed advantages over digital computation of Fourier transforms and downloading into a spatial light modulator for each reference image.

The optical correlator demonstrated in this program has potential DoD applications in object and target recognition, automated security systems, and image processing. The correlator is not limited to analog optical images, but can also be used with digitally encoded information such as radar and sensor data that is input through the SLM as a two-dimensional pattern. The resulting correlation results can then be used for functions such as guidance and control, automated target recognition, or image and feature analysis. In addition, commercial applications of the correlator in similar areas include industrial process inspection, document archiving and retrieval, holographic data storage, and security.

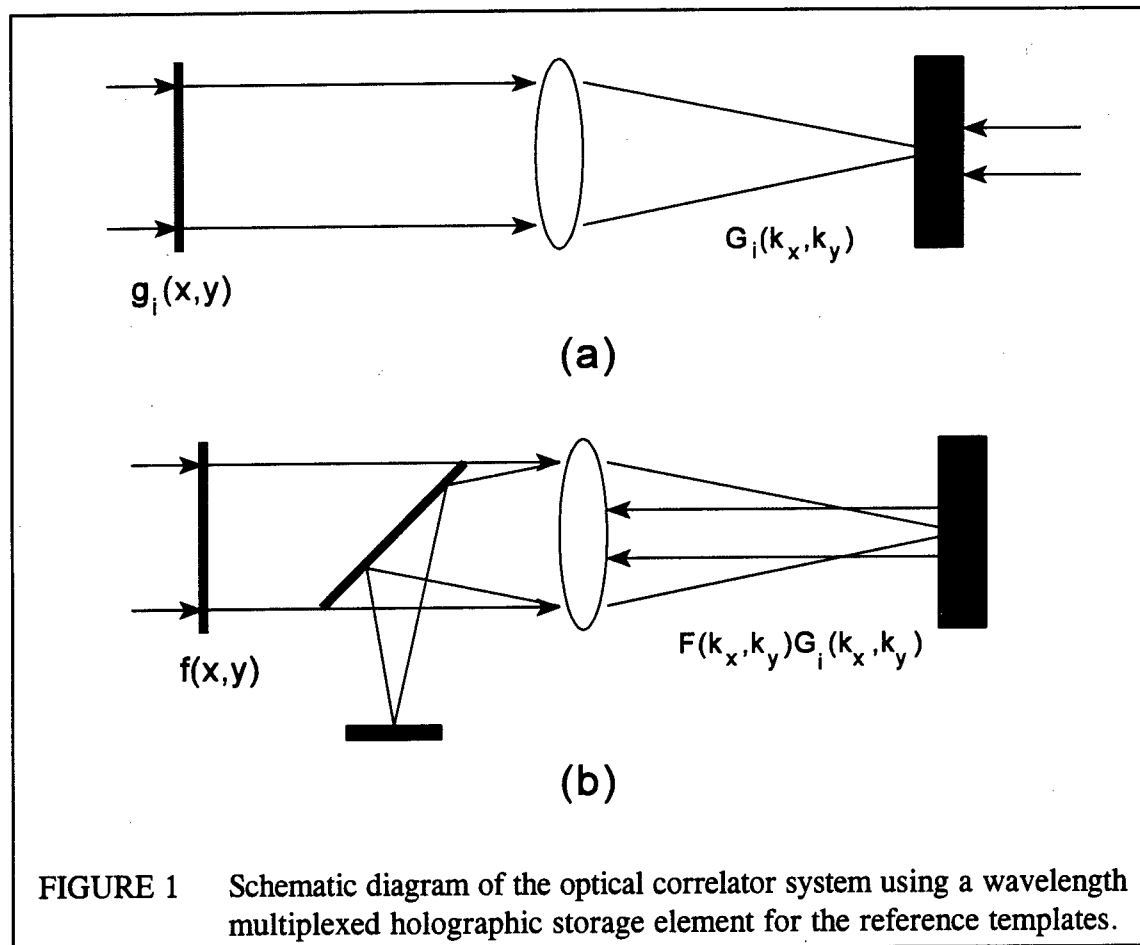
TECHNICAL BACKGROUND

Accuwave's optical image correlator combines Fourier optics with holographic storage to perform the correlation operation for a large number of images in a parallel accessing

format. Optical correlation is a fundamental operation of pattern recognition, where an unknown input image is compared against a set of known reference images stored in the system in order to identify and/or classify it. A holographic storage element, using the counter-propagating, wavelength-multiplexing architecture to preserve the high spatial resolution features of the stored images (i.e. their Fourier transforms), is used as the reference filter in the correlator system. To identify an unknown input image, correlations of the input and each of a large set of stored images are generated, and the best match is determined by the post-processor.

OPTICAL IMAGE CORRELATOR

The optical image correlator used in this program is based on the standard $4f$ VanderLugt correlator for multiplying the Fourier transforms of two images and taking the inverse Fourier transform.^{1,2} In our approach, a volume holographic element provides the multiple stored reference image templates. Figure 1 illustrates the recording and readout processes for the system, which relies on optical multiplication of the two images'



Fourier transforms through holographic readout. Since the reference filter operates in reflection, only a single Fourier transform lens is necessary. The stored templates are recorded as Fourier transform holograms at unique wavelength addresses, which are accessed by tuning the readout source. In the original in-house program at Rome Laboratory, a second SLM was used as the reference filter in the standard $4f$ configuration; however, this approach requires additional computation time and results in processing delays due to the necessity of downloading each reference image into the SLM. This delay becomes significantly larger for increasing numbers of stored images because the process would need to be repeated for each reference image.

In Accuwave's implementation of the correlator, the reference images are recorded into the system as Fourier transform holograms, as shown in Figure 1. During readout, the unknown input image is Fourier transformed and used to illuminate the holographic element at the wavelength addresses of each of the stored holograms, generating a product of Fourier transforms of the input and stored images:

$$\begin{aligned}
 h(x, y) &= FT^{-1} \left[F^*(k_x x, k_y y) G(k_x x, k_y y) \right] \\
 &= \frac{1}{(2\pi)^2} \int_{-\infty}^{\infty} \int_{-\infty}^{\infty} F^*(k_x x, k_y y) G(k_x x, k_y y) e^{i(k_x x + k_y y)} dk_x dk_y \quad (1) \\
 &= f(x, y) * g(x, y)
 \end{aligned}$$

where F and G are the Fourier transforms of $f(x, y)$ and $g(x, y)$, respectively. The optical generation of the Fourier transforms and inverse transforms and wavelength-addressed storage of the reference templates provides considerable speed advantage over computer generation of the two-dimensional image correlation of the input image and every stored template.

WAVELENGTH MULTIPLEXED STORAGE

Of the two major approaches used today for holographic storage, wavelength multiplexing enables holograms to be recorded in the optimum geometry for high resolution storage. This approach uses the counter-propagating geometry, where the large field of view of the grating enables images with high spatial frequency content to be recorded with minimal crosstalk. Multiplexing with wavelength enables a simple source tuning action to be used to access all of the recorded holograms, instead of a complex system of optics and electro-optic beam deflectors that would be required for angle multiplexing.

The counter-propagating geometry was initially reported by Accuwave Corporation as a means to provide maximum spectral selectivity and maximum angular field of view,

which translates into being able to store high resolution images with minimal inter-page crosstalk. The spectral width for a reflection hologram is given by:

$$\Delta\lambda = \frac{\lambda^2}{2n_0\ell} \quad (2)$$

where $\Delta\lambda$ is the FWHM bandwidth, λ is the wavelength, and ℓ is the thickness of the grating. The field of view is given by

$$\frac{2\pi n_0}{\lambda} \left[\sqrt{1 - \frac{\cos^2(\varphi - \Delta\varphi)}{n_0^2}} - \sqrt{1 - \frac{\cos^2\varphi}{n_0^2}} \right] = \frac{\pi}{\ell} \quad (3)$$

for a reflection grating, where φ is the angle of reflection of the grating ($\varphi=0$ for counter-propagation) and $2\Delta\varphi$ is the field of view (full angle). As an example, a 4 mm thick, $\lambda=650$ nm grating will have an angular field of view (full angle) of about 2° .

Large field of view is advantageous in the correlator application for recording high feature resolution (resulting in exact reproduction of the Fourier transform of the various images). In addition, the field of view also provides translation invariance, where changes in the input image position results in angular changes at the holographic grating (i.e. in the Fourier transform plane) that must be within the field of view of the grating. A narrow field of view would result in a drop-off in the correlation signal output as the object moves away from its original position. This feature can be used for image tracking as well as correcting for positioning errors and variations in the image input. Storage of 500 high resolution holograms (i.e. with feature size of less than $5 \mu\text{m}$) has been demonstrated. Inter-page crosstalk was negligible with hologram separation of 0.4 \AA (where FWHM bandwidth of the grating was 0.1 \AA).⁴

TUNABLE LASERS EVALUATION

Wavelength multiplexed holographic recording and readout necessitates use of tunable lasers. For recording the holograms in the reference element, a tunable dye laser using DCM Special dye was to be used. During readout, the same wavelengths were to be generated using a tunable external cavity semiconductor laser, which provides a compact, low power consumption source with about 10 nm of tuning range in the visible (around 650 nm). Recently, lasers with center wavelengths at increasingly shorter wavelengths, i.e. approaching 630 nm, have been reported.

Rome Laboratory has a tunable external cavity laser that was built by Micracor with a center wavelength of 653 nm, which was used in a previous optical image correlation

demonstration. Maximum output power of 3 mW was obtained near the center wavelength. The manufacturer has since discontinued the visible laser, making future support uncertain. For this reason, along with the recent advances in tunable lasers and new manufacturers entering the market, we evaluated some of these new entrants for possible use as the correlator readout source.

NEW FOCUS. New Focus introduced a tunable visible laser at CLEO 1995, using the piezoelectric driver to operate the tuning grating. This laser has overcome considerable delays due to the need to develop a process for anti-reflection coating the Fabry-Perot laser used as the gain element. The coarse tuning mechanism is operated by their piezoelectric screw driver, which is limited in maximum speed (taking several tens of seconds to tune over its 10 to 15 nm wavelength range) and lifetime of the piezoelectric elements (which is approximately 1,000 to 1,500 hours at full tuning speed). Therefore, the laser appeared to be designed for occasional wavelength changes and not a continuing scanning mode that would be required for the correlator application.

ENVIRONMENTAL OPTICAL SENSORS. Environmental Optical Sensors, Inc. (EOSI), a small company in Boulder, Colorado, has also developed a tunable laser in 1995 and has offered an improved model for delivery starting in early 1996. This laser uses a mechanical actuator to drive the tuning element, which is more suited for continuous wavelength scanning. The laser elements are inter-changeable using a common cavity. However, the laser has been plagued by manufacturing problems and deliveries have been delayed several months. This laser was planned as an alternate to the Rome Labs Micracor laser, which required extensive repair by the manufacturer (who no longer manufactures this particular laser), but was not available in time to be used for the correlator demonstration.

SDL. SDL has announced development of a tunable external cavity semiconductor laser with output powers in the 100's of mW at 670 nm, but this laser is not expected to be ready for delivery until some time next year. The NIR version of this laser is currently being delivered.

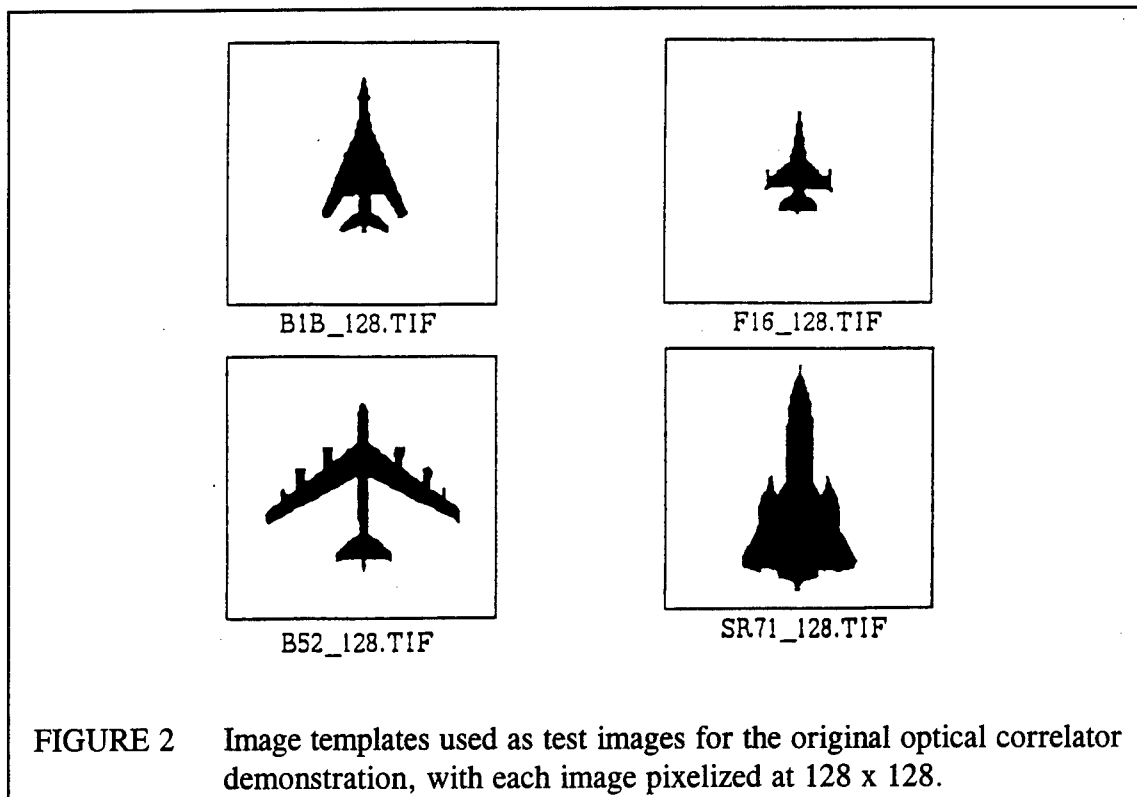
After evaluation of the available tunable laser options, we decided to continue with using the Micracor laser at Rome Laboratory as the best option at this point. Using the automated computer control features of the laser would provide adequate capability for demonstrating the correlator. The laser and other elements of the correlator system would be controlled and monitored using LabView.

During initial testing, the Micracor laser diode element and tuning mechanism failed at Rome Laboratory and necessitated repair at the factory. This took longer than expected due to the unavailability of parts. Although the gain element was replaced (with one for

a different wavelength due to unavailability of laser elements at the original wavelength), continuing problems with the actuator (that prevented the laser from tuning) precluded use of this laser in the correlator demonstration at Rome Laboratory. Therefore, the demonstration was done at Accuwave using the Coherent 899-29 laser as the source. The readout was done with the laser power attenuated to a power level comparable to that of the tunable semiconductor lasers, i.e. a few mW output.

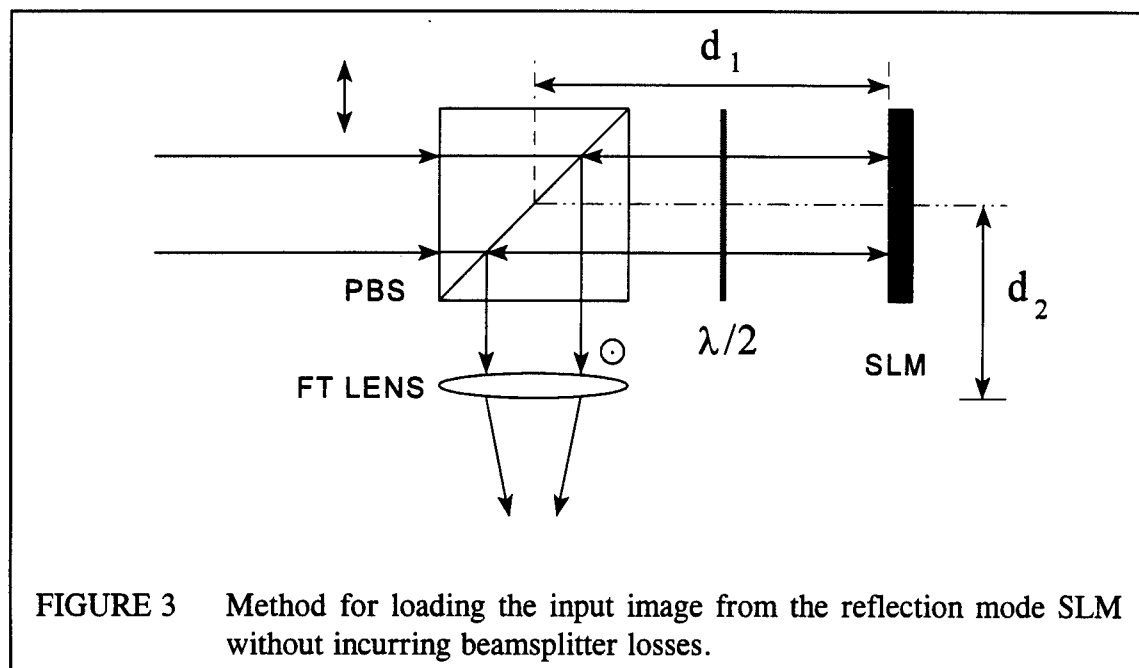
SPATIAL LIGHT MODULATOR INTEGRATION

The first task in this program was integration of the new BNS SLM into the previously demonstrated correlator system so that it can be used to input the test images for readout. Use of a spatial light modulator in the correlator system will enable real-time operation of the system with a given input image, as well as enabling larger numbers of test images to be attempted. In the previous experiments, high contrast transparencies were substituted for the SLM to demonstrate the concept. Now, an SLM carrying the same images on the transparencies would be used for readout. The transparencies were to be retained for recording because of their ability to tolerate higher optical throughput that would be necessary for holographic recording using relatively high power sources. The original image was pixelized to match the dimensions of the Semetek SLM at Rome Laboratory, as shown in Figure 2.



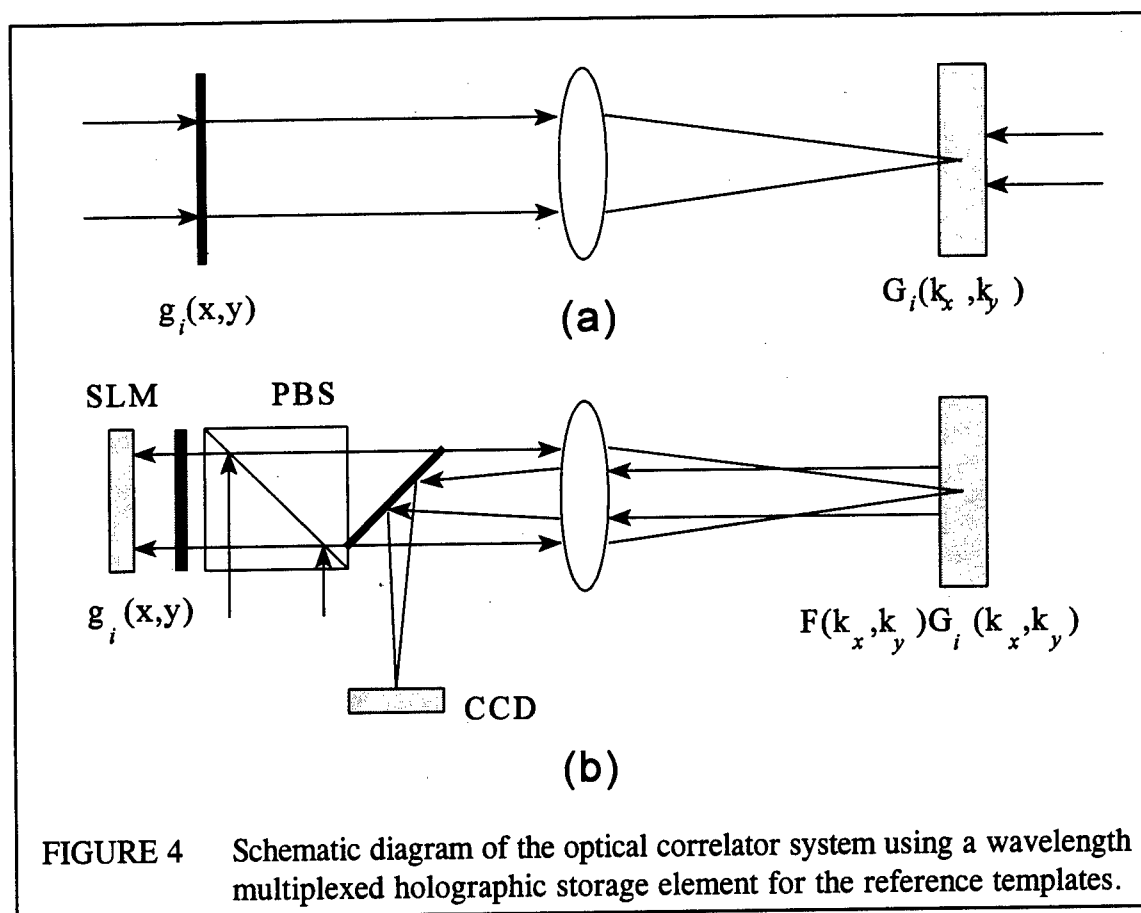
BNS SLM SETUP

Rome Laboratory had ordered a Ferroelectric Liquid Crystal Spatial Light Modulator from Boulder Nonlinear Systems in Colorado for use in this program. The key feature of this SLM was the high throughput (10%), which is an order of magnitude more than the Semetex SLM's that had been used in the Lab in the past.⁵ The SLM was delivered to Rome Laboratory in the Fall of 1995 and tested using the existing transparency as the input images, which had the same pixel pitch as the SLM. Since the SLM was a reflection device, the optical layout shown in Figure 3 was used to enable the back-reflected signal to be accessed without incurring 75% beamsplitter losses (from double passing through a 50/50 beamsplitter). A simple model for the SLM is a variable polarization rotator, with rotation angle α ranging from 0 to $\pm 22.5^\circ$.



The SLM operation is cycled through an alternating positive and inverse image format by the drive electronics so the average state is zero. This is necessary to avoid poling or charge buildup on the liquid crystal material, which will eventually pole the SLM substrate material and adversely affect proper operation. Although this cycling can be accommodated in the software, the need to maintain this type of operation is an added complication for routine operation of the correlator that should be considered in evaluating it for actual system application. Moreover, the reflection mode operation of the SLM adds issues of surface reflection from both the front element and the backplane of the device.

The experiment setup for the optical correlator, with recording using a transparency and readout with a reflection SLM, is shown in Figure 4. The transmission photomask is used for recording (Figure 4(a)); the photomask is then substituted with the SLM and associated optics for readout (Figure 4(b)). This enables high power to be used during recording, while enabling large numbers of test images to be loaded into the correlator in real time for readout. However, the contrast in correlation patterns (i.e. auto- vs. cross-correlations) for different input images against a given reference was low. This was determined to result from the non-unity fill factor of the BNS SLM, which can be seen in the microscopic enlargement of the pixels shown in Figure 5. The pixel dimensions are approximately $22\text{ }\mu\text{m}$, with a center-to-center pitch of $30\text{ }\mu\text{m}$. This results in a 54% fill factor, where the spatial period of the Fourier transform components from the individual pixels is different from that obtained from a full pixel (with a 100% fill factor) image, resulting in the low auto-correlation results. As a result, a new transparency was fabricated, incorporating pixelization into the image pattern so the exact pattern of the image from the SLM is duplicated.



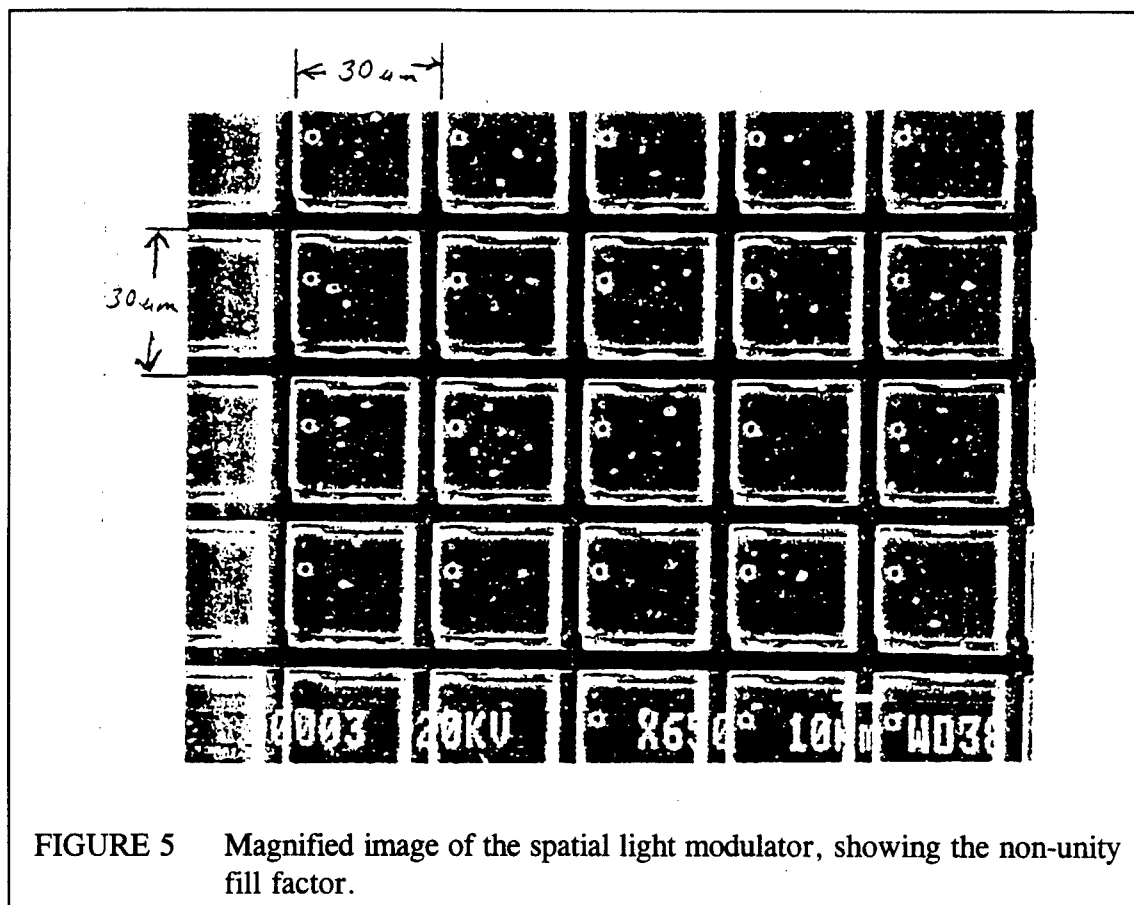
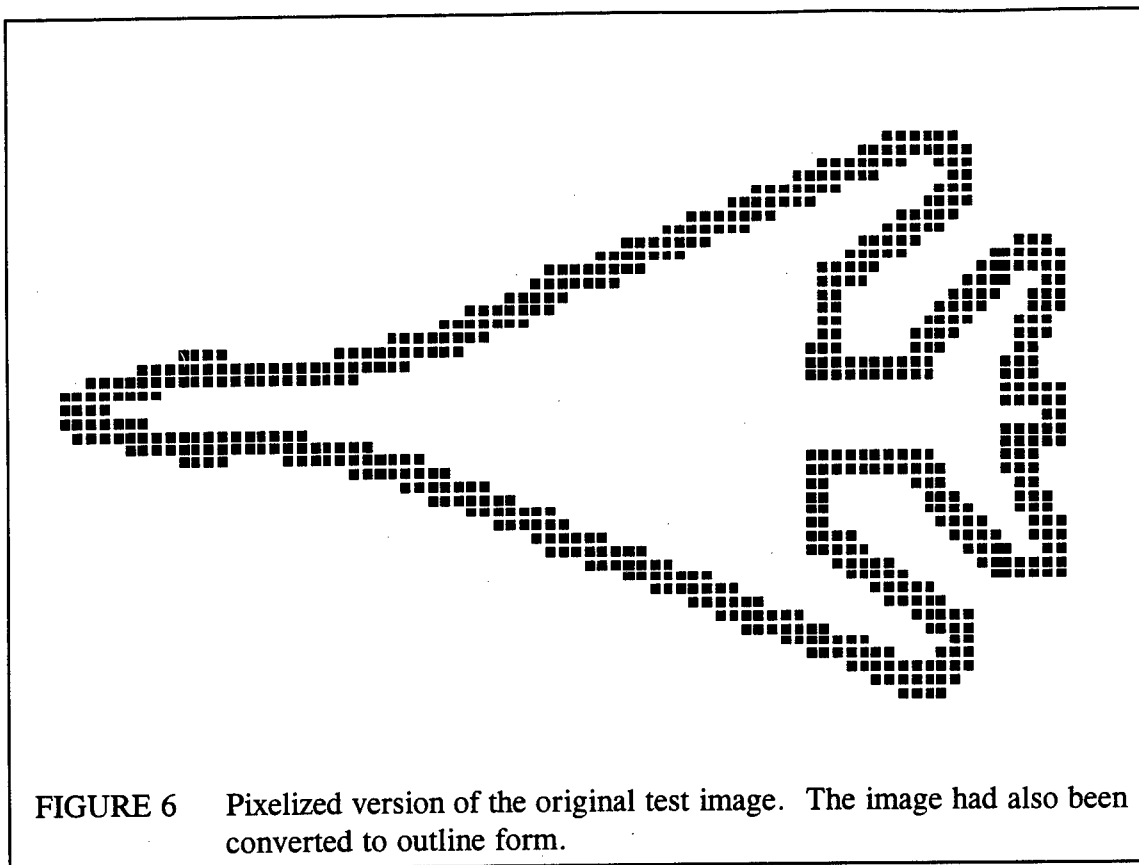


FIGURE 5 Magnified image of the spatial light modulator, showing the non-unity fill factor.

IMAGE FORMATTING

The original images used for recording the Fourier transform reference filters for the correlator were full pixel images, at 128×128 pixel resolution. However, the BNS spatial light modulator (SLM) had a $22 \mu\text{m}$ square active area but with $30 \mu\text{m}$ separation. When the recorded Fourier transform holograms were used with the SLM for readout, the difference in spatial period of the Fourier transform of the SLM image resulted in poor correlations. Therefore, a properly formatted image was made using a modified version of the mask pattern generation program that we had used before.

Figure 6 illustrates an example of an image generated using this new approach. A custom program was created to replace the full size pixels of the original image with pixels of any specified dimension while maintaining the same pitch. The output was formatted as an AutoCAD.dxf file that can be loaded directly into the photomask pattern generator. Both full images and outlines of these images were used. The outline pattern was also investigated to see if this would reduce the strong DC term that is present in the correla



tion output. A new chrome on glass transparency was fabricated using these new image files.

SIMULATIONS

Simulations of the correlation operation were made using the original reference image transparency and the SLM, and also with the new pixelized images. The latter case was done using a 512×512 format, where a 4×4 grid was used to represent one pixel. The fill factor with 9 active sub-pixels is 56%, which is almost exactly the measured fill factor of the SLM.

The result of correlating the full pixel image to its pixelized counterpart with the simulation program was similar to the auto-correlation distributions observed in the initial experiment (with the low auto-correlation levels due to the improperly matched pixel dimensions). However, a much better match resulted when the new input images were used in the simulation. Based on these results, the "pixelized" pattern was used to generate a new image photomask, which will be used with the SLM-input image during readout.

SLM BASED RECORDING AND READOUT

The pixelization pattern problem can also be avoided by using the same type SLM to record the image as well operating the image correlator. This will require an SLM with sufficient contrast at the higher optical power used for efficient recording. As an initial feasibility experiment, the recording and readout setup of Figure 4 was modified to enable the signal from the SLM to be used to record the hologram as well as reading it out. In this setup, the PBS also enables the object and reference beam intensities to be redistributed without throwing away any power. However, when recording was attempted with the BNS device, saturation of the pixel elements reduced contrast of the binary image at illumination intensities of $> 1 \text{ mW/cm}^2$. This limitation severely restricted use of this device to that of readout only under low power illumination. However, an alternate solution was developed, making use of one of the new liquid crystal displays from Kopin Corporation.

KOPIN SLM IMPLEMENTATION

Kopin Corporation has recently introduced a liquid crystal VGA display that was being used by the data storage research community as an image input device. Accuwave had recently obtained the LCD test kit for a similar application, and we also investigated the suitability of using this as the input SLM in the optical correlator. Contrast ratio was quoted as better than 100:1, with the device designed for projection applications where it will be illuminated with high intensity light. As a result of testing this device, we concluded that this SLM provides considerable advantages in the optical correlator application for the following reasons:

- The Kopin LCD is currently available on the commercial market, with a list price of about \$3,000, which is considerably less than the purchase price of a commercial SLM system;
- It has a higher contrast ratio between the on and off pixels and ability to withstand higher illumination intensity, which is essential when using the SLM for recording as well as readout;
- The device operates in transmission, eliminating the need for additional optics (with added complexity and absorption losses) to pick off the back-reflected signal and directing it into the correlator;
- The Kopin LCD is formatted for standard VGA (640 x 480 pixel), providing higher resolution than the BNS FLC and simplifying interfacing with a computer using existing software.

This latter feature was used advantageously in the correlator demonstration by using the standard Microsoft PowerPoint program to drive the SLM with various test images. It also simplifies writing customized code for operation of the system by relying on standard screen commands.

REFERENCE IMAGE RECORDING

The correlator system as shown in Figure 7 was implemented using the Kopin LCD as a spatial light modulator for both image input and readout. The incoming light from the laser is split by the beamsplitter to serve as the object and reference beams. The $\lambda/2$ plate is used to rotate the polarization of the incoming beam by 90° so the object wave incident on the SLM has the correct orientation. A polarizer is attached to the back surface of the SLM to generate the amplitude modulated image. A 180 mm focal length doublet lens was used to generate the Fourier transform optically at the plane of the crystal. The reference wave is directed to the opposing face of the crystal by the mirrors to record the grating.

Wavelength multiplexed holograms of the reference image Fourier transforms were

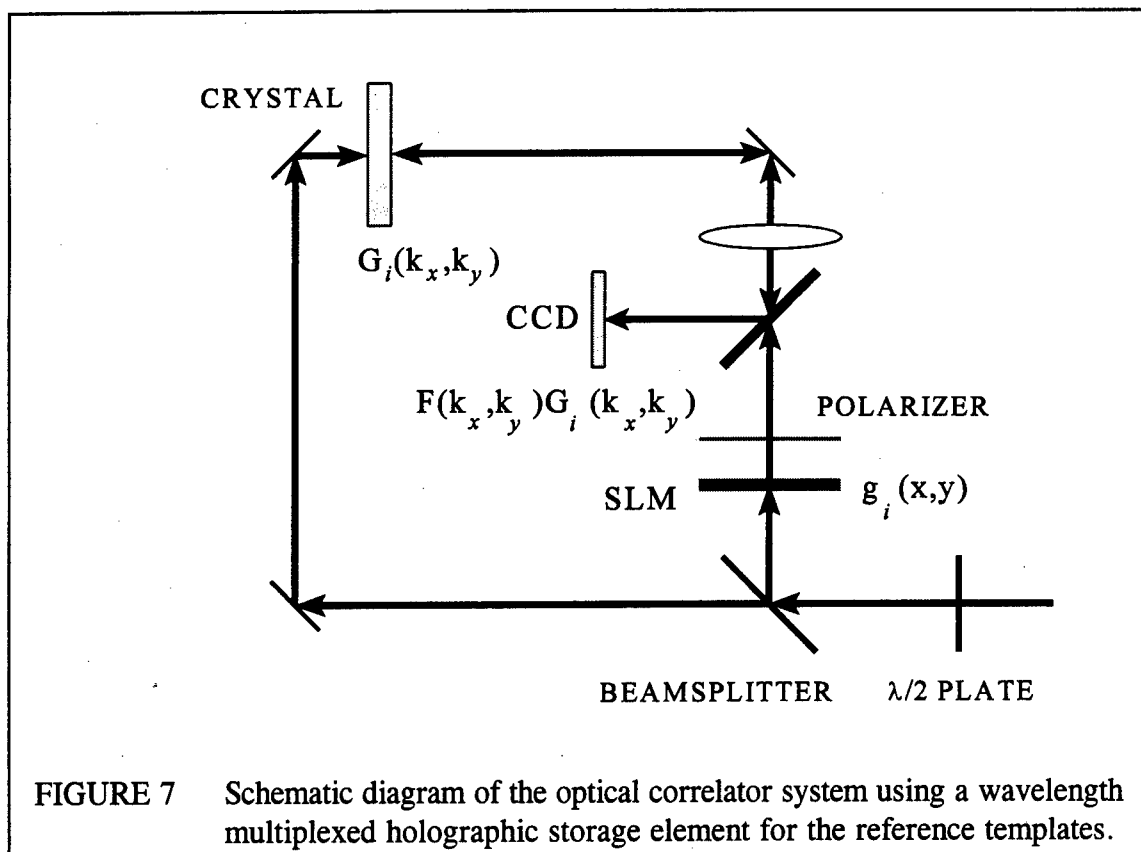


FIGURE 7 Schematic diagram of the optical correlator system using a wavelength multiplexed holographic storage element for the reference templates.

recorded in the LiNbO_3 crystal in the manner shown in Figure 7 at each wavelength address using a suitable exposure schedule (with gradually decreasing times for later exposures) to compensate for optical erasure of the initial holograms by subsequent exposures. A tunable dye laser, configured for operation in the 650 to 670 nm wavelength range (where tunable semiconductor lasers are currently available), was used for recording the holograms and readout. A photograph of this setup, with the main components of the correlator mounted on a self-contained breadboard, is shown in Figure 8. The input light can be fiber-coupled to simplify alignment with different sources.

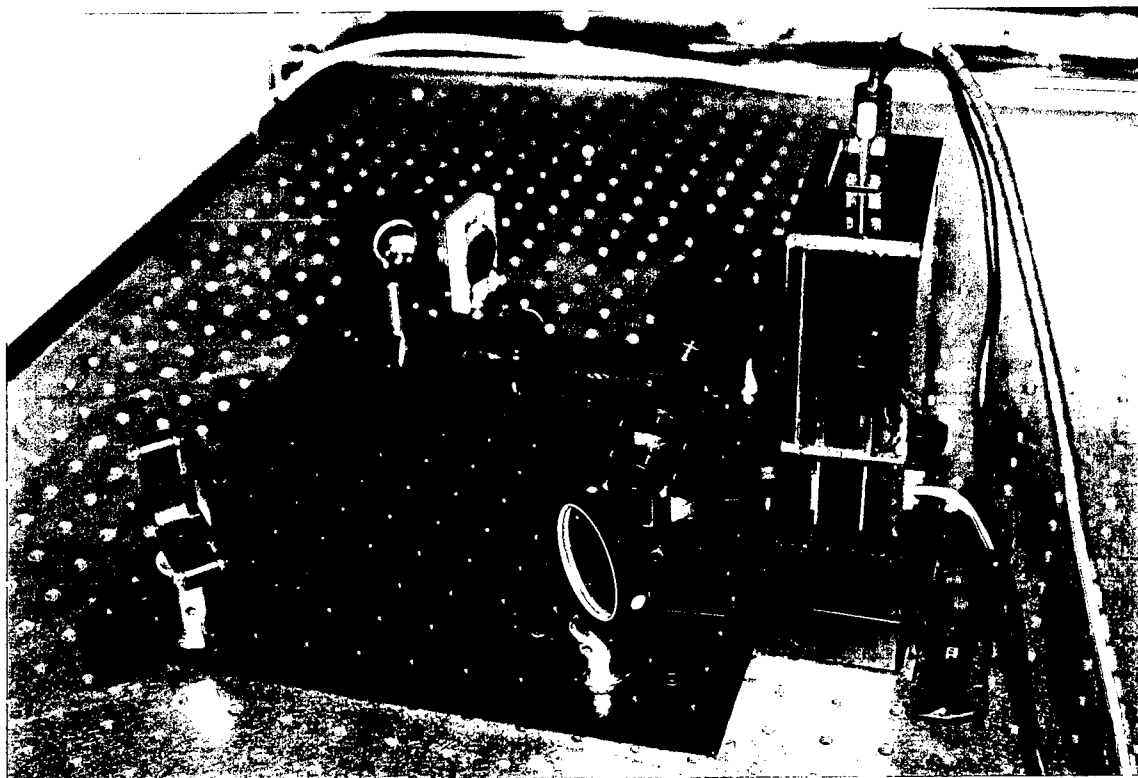
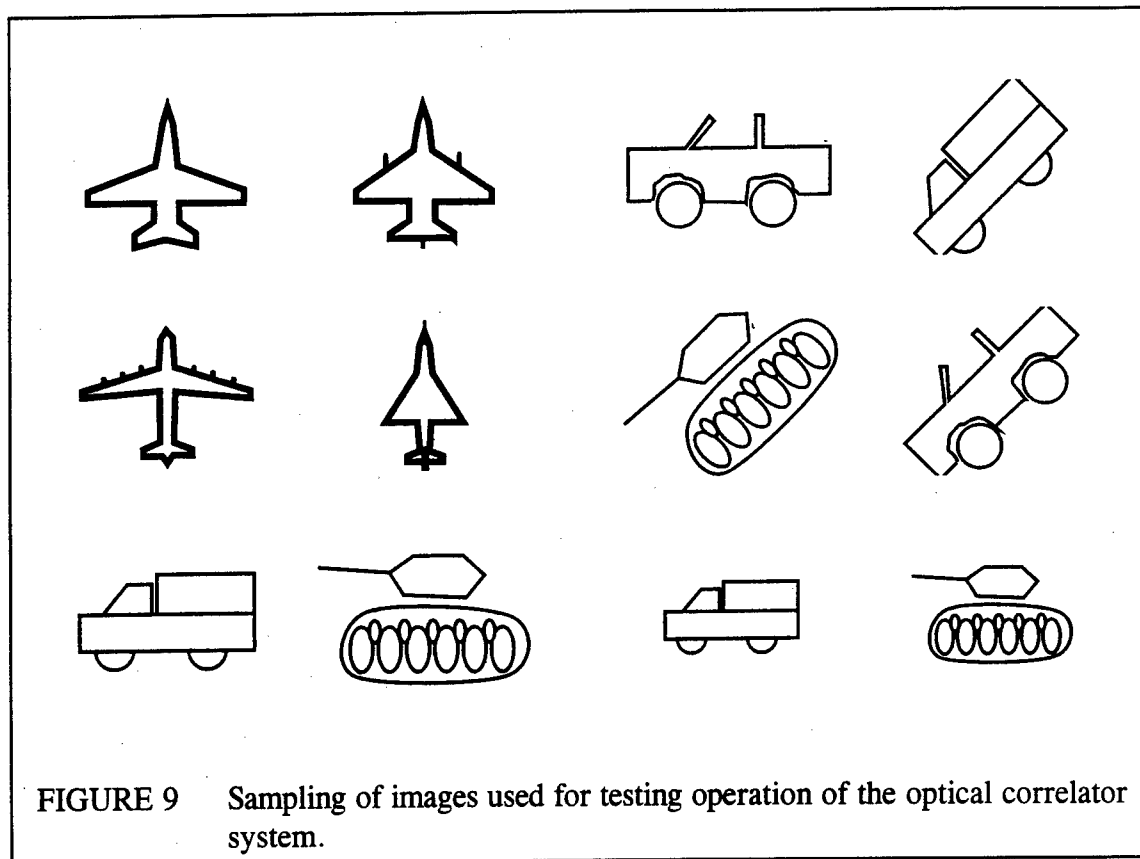


FIGURE 8 Photograph of the correlator breadboard in the laboratory, using a Kopin liquid crystal SLM as the input image source.

A set of test images were generated using a standard drawing and presentation program and displayed using a laptop computer (with the capability of displaying on both the built-in screen and through an external VGA port). Microsoft PowerPoint was used in screen presentation mode to drive the Kopin LCD with the test images that were sequentially loaded into the correlator for both recording and readout. Variants of each pattern, including slight changes in dimensions, scaling, and rotation, were used to generate a number of unique objects that were then recorded into the correlator's holo

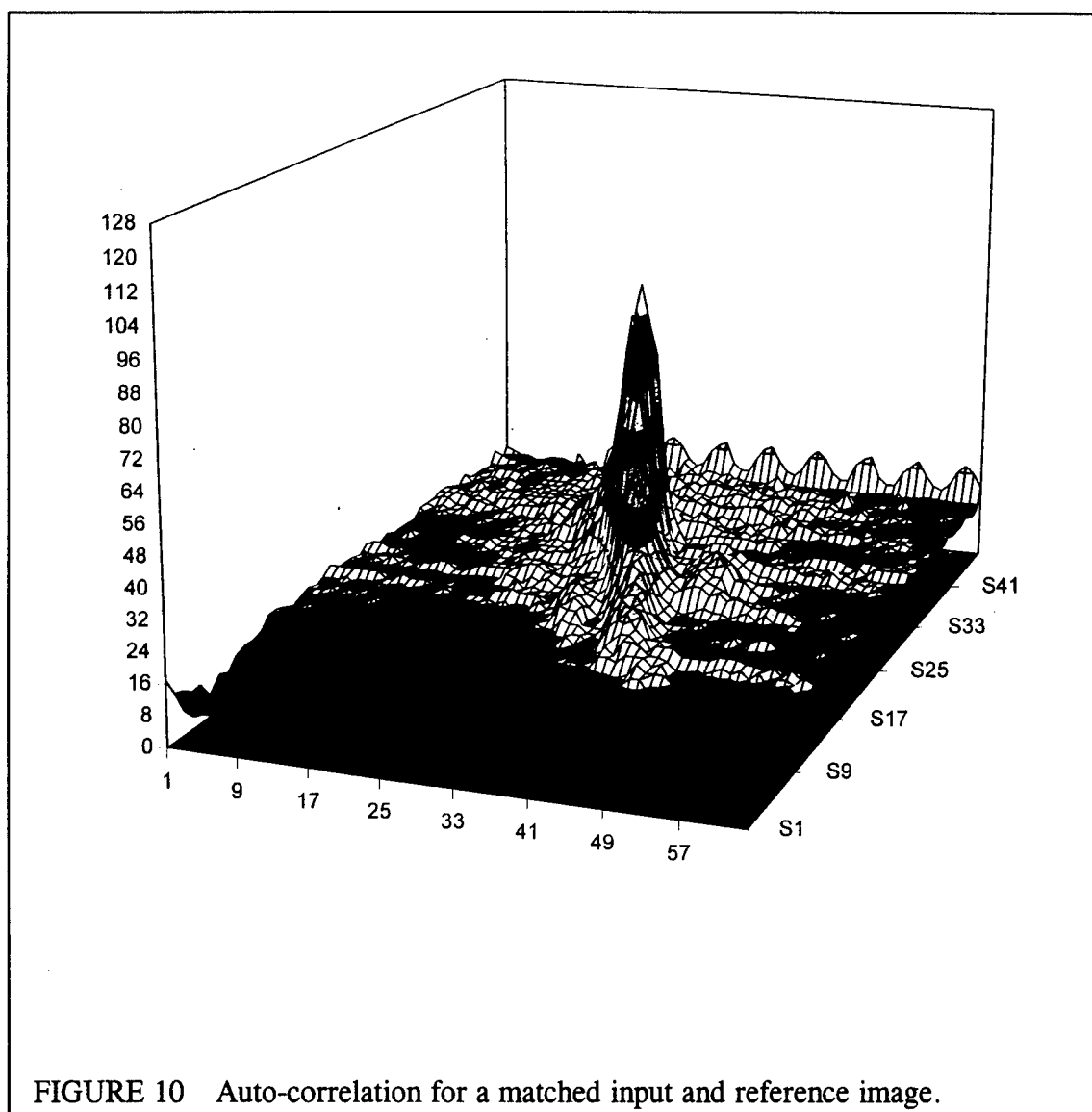
graphic element as the reference image templates. The images were formatted in outline form to reduce the DC background in the Fourier transforms and in the correlation. This resulted in a reduced grating modulation index due to the weaker object beam (since most of the image field is dark). A sample of these images, including scale and rotational position changes, are shown in Figure 9; the images are shown in inverse format, with the actual image on the SLM having a dark background.

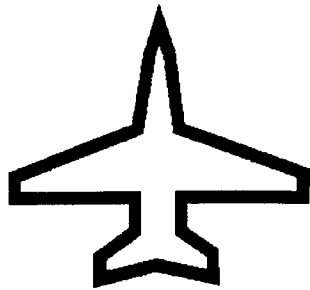


Twenty-five holograms were recorded over a 10 nm tuning range with wavelength separation of 3 \AA , taking advantage of the birefringent filter mode spacing of the dye laser. Each wavelength address corresponded to a unique stored image. Among the holograms, a pair of adjacent images was also recorded with 0.3 \AA separation to demonstrate the ability to record the gratings close together without crosstalk effects. No problems of SLM saturation or reduced image contrast were observed with the Kopin SLM, even with recording beam power of $> 100 \text{ mW/cm}^2$. Exposure energies were scheduled according to a nonlinear function to approximately equalize the auto-correlation peak intensities by compensating for optical erasure of the initially recorded holograms by subsequent exposures.

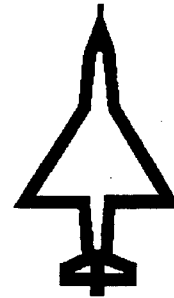
EXPERIMENTAL RESULTS

Auto- and cross-correlations of similar and dissimilar images were compared to determine the difference in their correlation outputs and the contrast in the correlation as a means for determining image matching. A specific input image was selected for display on the SLM, and the wavelength was tuned to obtain correlations against a range of reference images. The correlation output at the CCD detector was transferred to a frame grabber and plotted in 3-d form to obtain a clear picture of the peak intensity and intensity distribution. These results are shown in Figures 10-12, which are auto- and cross-correlations of images of the type shown in Figure 9.

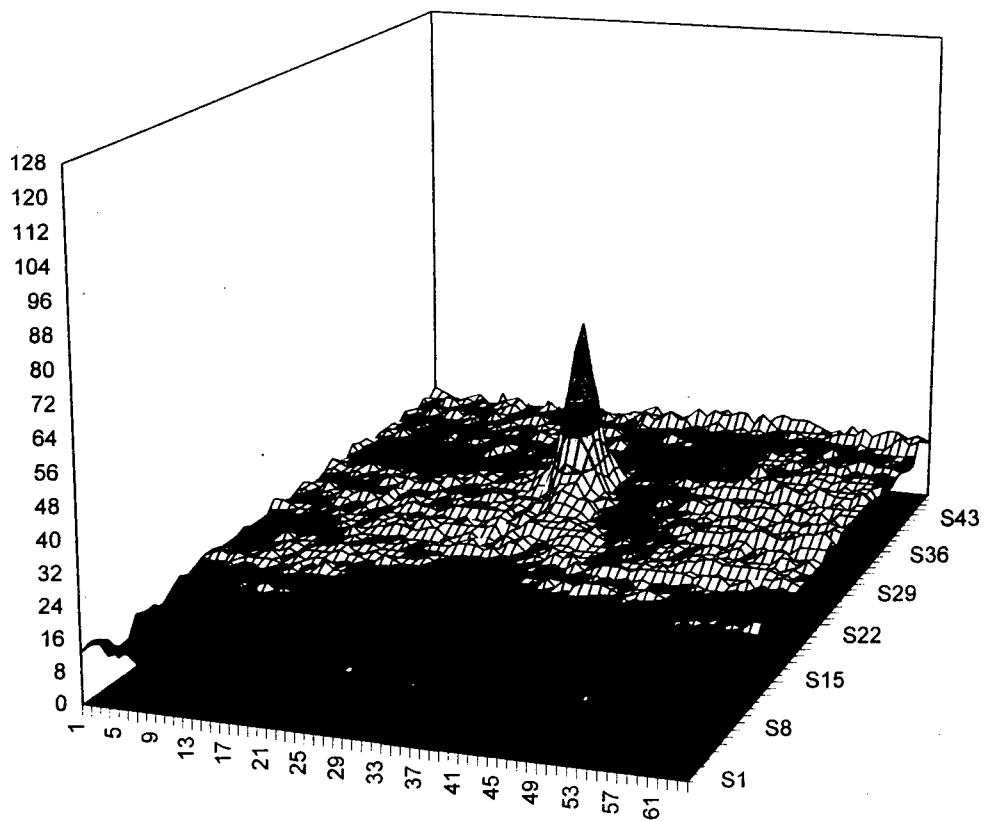




(a)



(b)

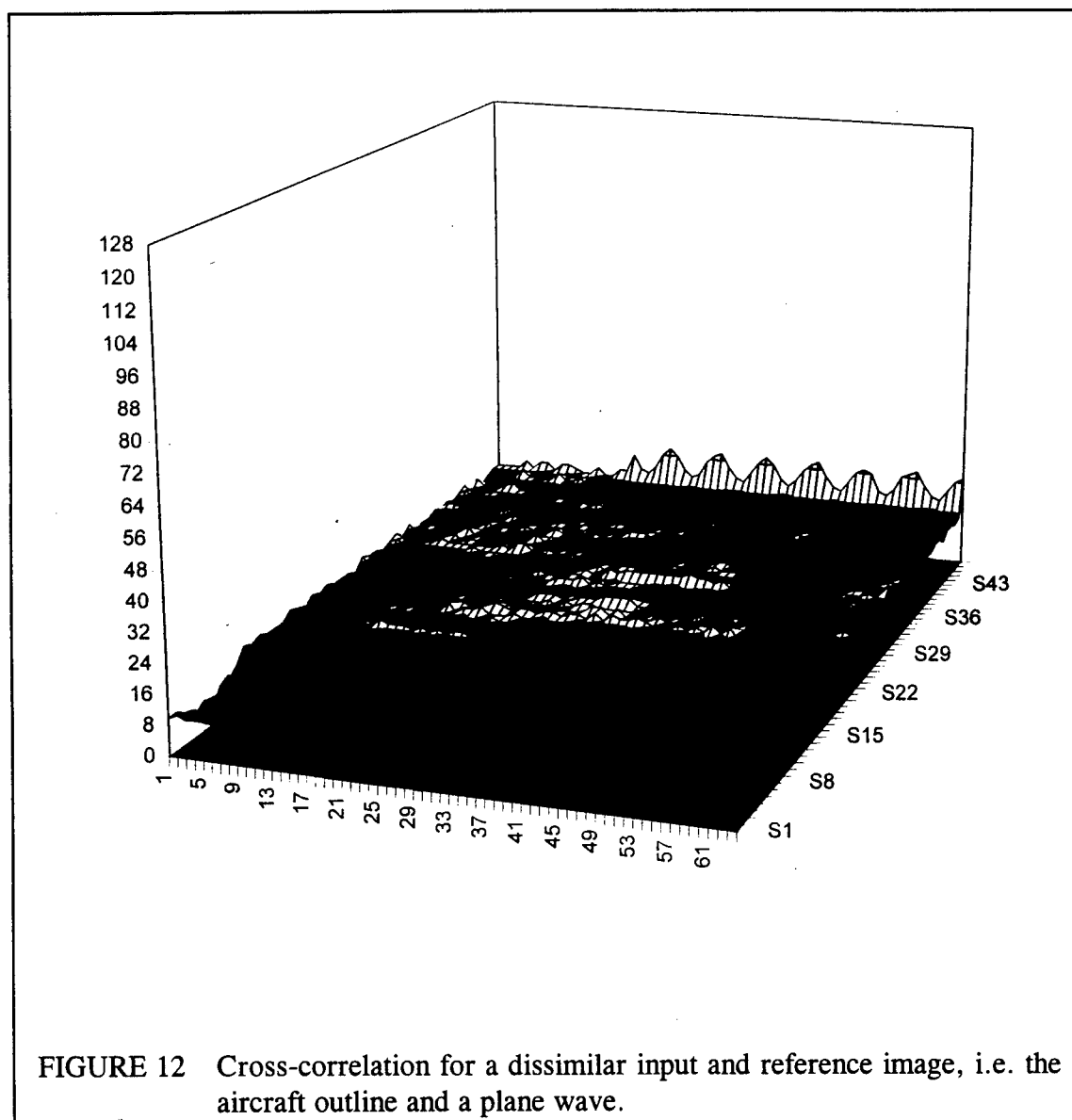


(c)

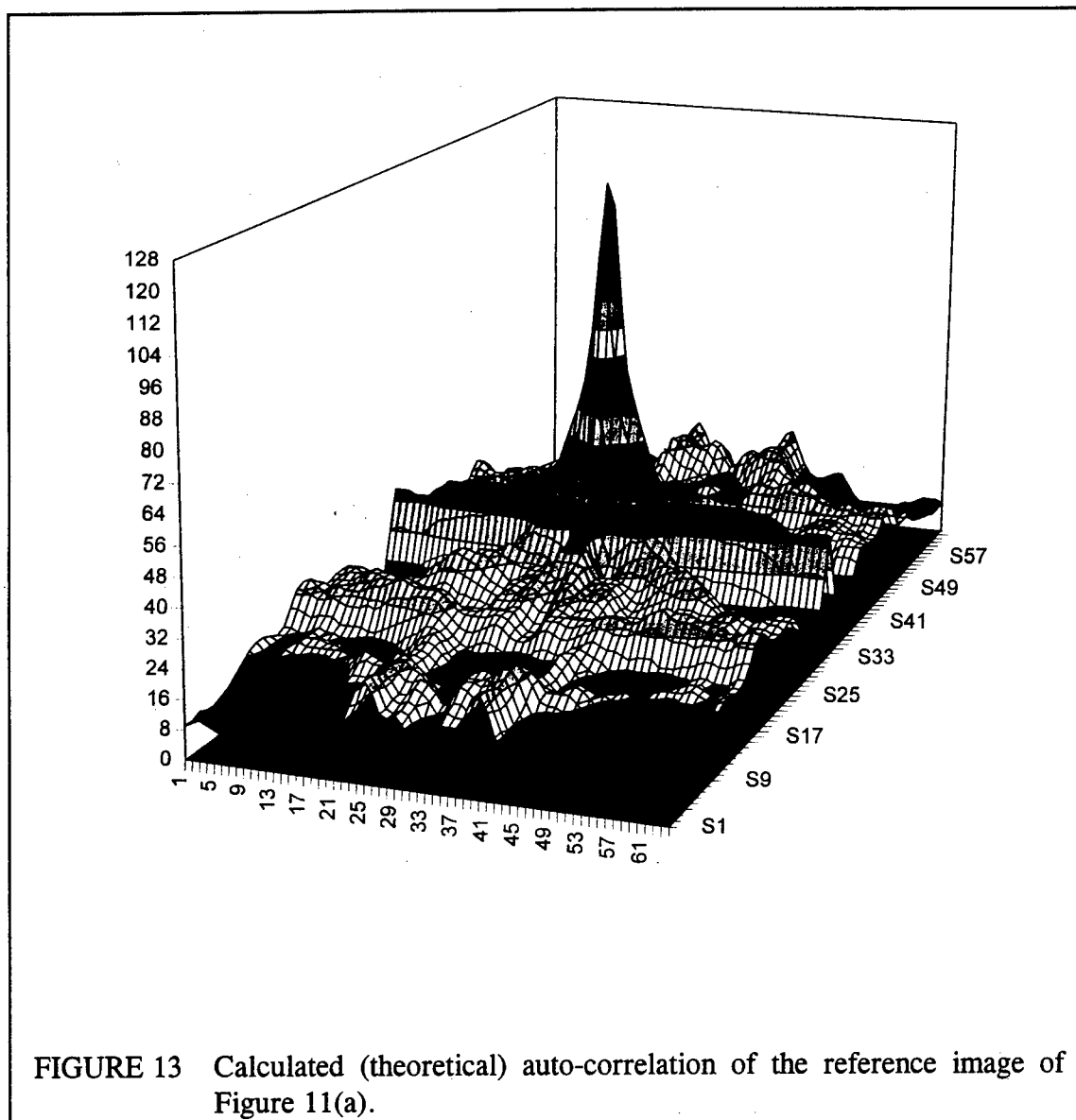
FIGURE 11 Cross-correlation output for pair of similar shape but different images; (a) images used, and (b) correlation output.

In Figure 10, the auto-correlation, where the input image and reference image accessed at that particular wavelength are identical, is shown. The test image (shown in Figure 11(a)) was one of the 25 stored in a wavelength multiplexed volume holographic element using the techniques described earlier. The wavelength was tuned to access the identical stored reference image to obtain the auto-correlation. The correlation output was recorded and analyzed using a frame grabber and three-dimensional plotting algorithm to show the contours of the output signal as well as the peak intensity.

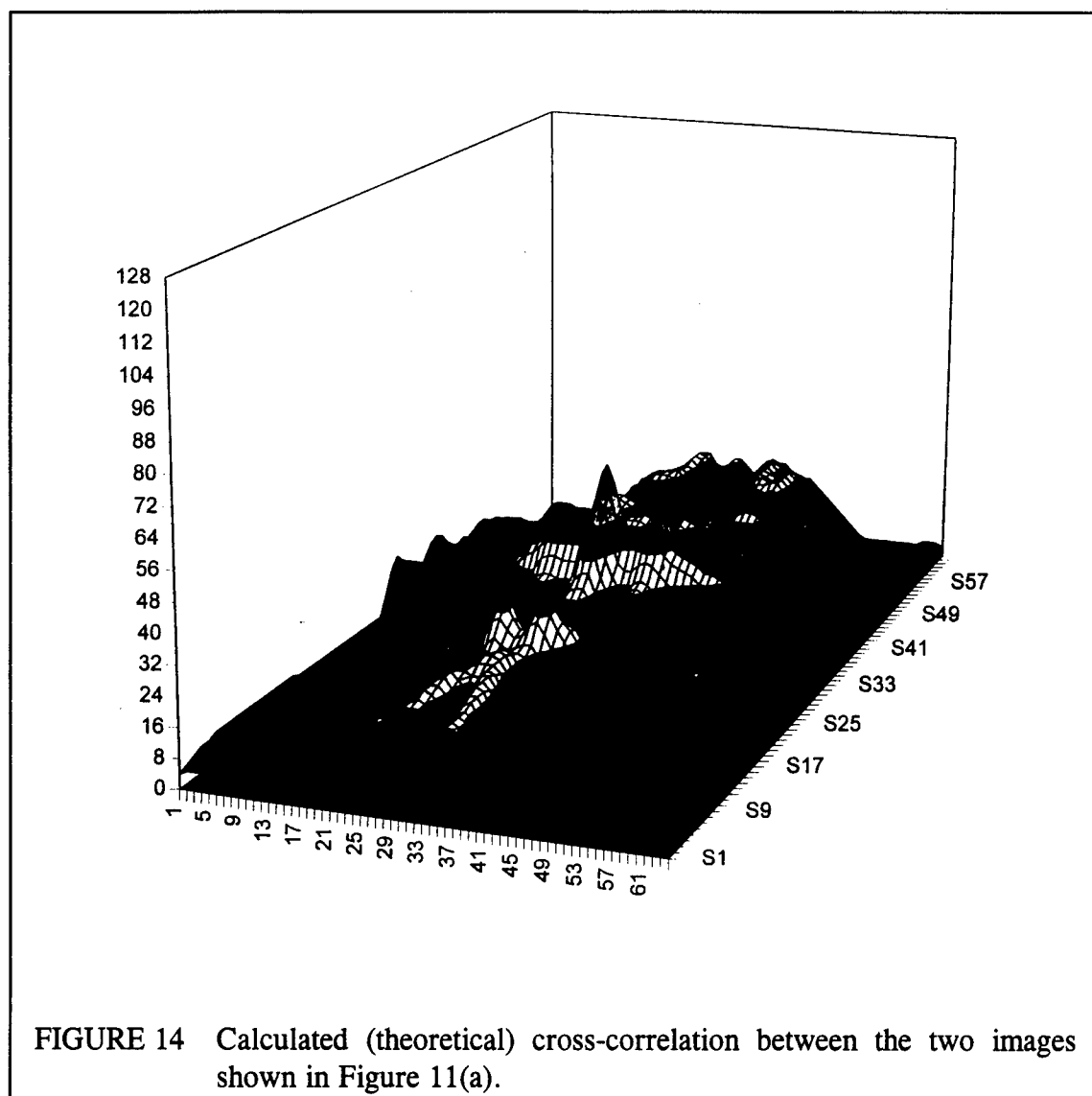
For the cross-correlation results shown in Figure 11, an input image that is slightly different in shape from the reference image was used to test the ability for the correlator



to differentiate between the two. The new input image, shown in Figure 11(b), is another aircraft outline, but with slight changes in the wing area, shape, and aspect ratio compared to the reference image in Figure 11(a). The correlation between these images is shown in Figure 11(c), where the difference between the two images is indicated with a correlation peak of reduced amplitude and slope from that of the auto-correlation. In comparison, Figure 12 shows the correlation between the aircraft and a totally dissimilar image (i.e. with an unmodulated plane wave). For this case, the overall cross-correlation output has a considerably lower amplitude than the case in Figure 11(c), with the peak being barely discernable.



These experimental results from the optical correlator were in close agreement with computer simulations using the same test images, indicating that the error as a result of optical implementation of the Fourier-transform and inverse Fourier transform and in holographic recording and readout of these patterns is small. This is partially attributable to the high storage fidelity of the holographic element and the result of using an exact, optically generated Fourier transform to generate the correlation. The theoretical auto-correlation of the outline image in Figure 11(a) and the cross-correlation of the images in Figures 11(a) and (b) are shown in Figures 13 and 14, respectively. Their close resemblance of these and the experimental results indicate the relatively high fidelity of this optically-based approach.



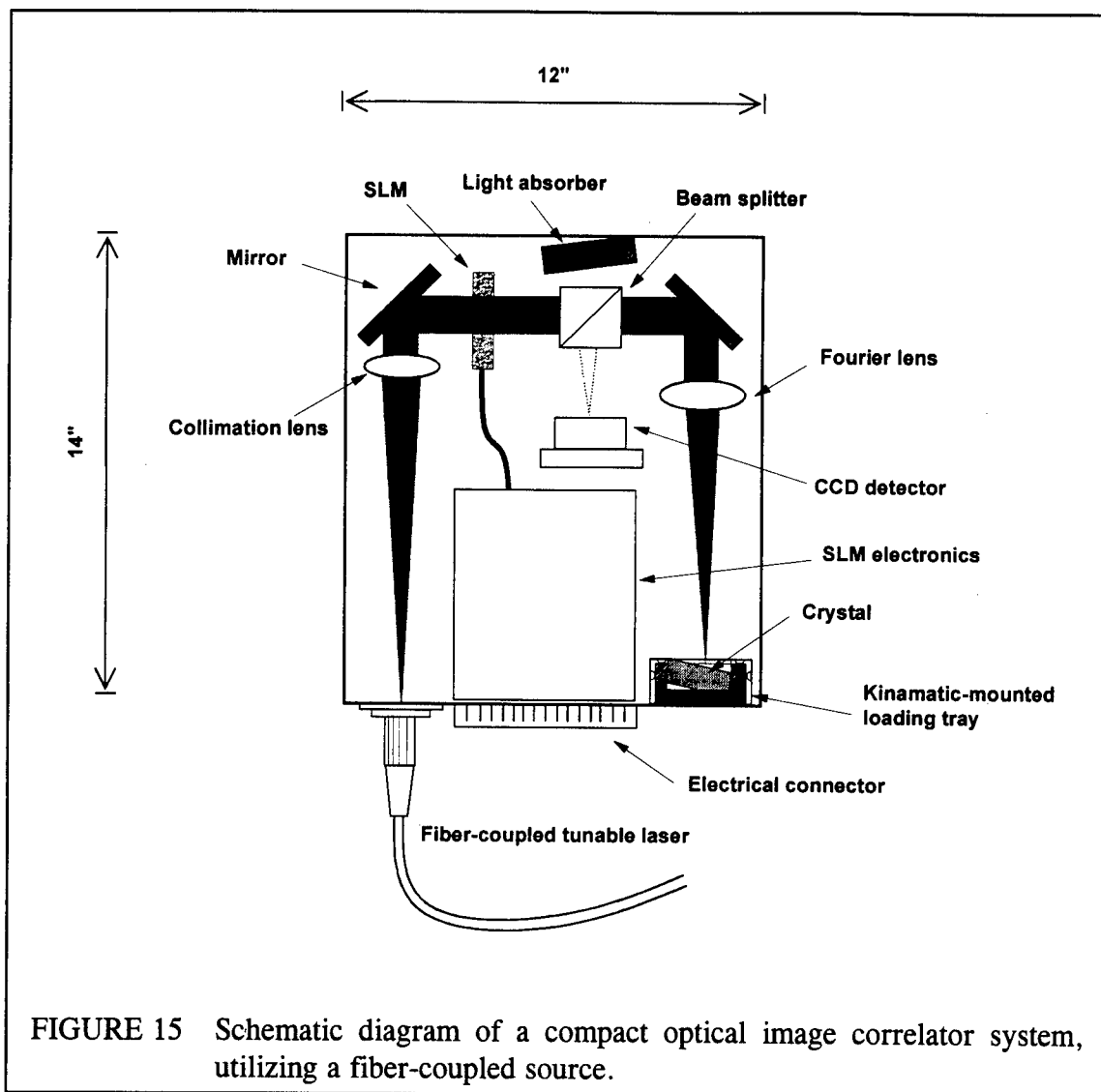
COMPACT OPTICAL CORRELATOR SYSTEMS

Based on the results demonstrated in this program, a compact, self-contained optical image correlator system is feasible. The ability to use the SLM for both reference image recording and correlation readout enables programming of the correlator to be done in real time, bypassing the time and costs required to fabricate master transparencies for recording. Moreover, there will be no issue of pixel matching between the recording transparency and the readout SLM. Compact SLM's are now available, as shown by the one used in Figure 8. The proper choice of optics and fabrication on a customized optical bench can further reduce the package size.

Figure 15 illustrates a concept for a compact optical correlator system, where the unit utilizes an external fiber-coupled source. The fiber-coupling eliminates the need for re-alignment of the system due to small shifts in incident beam direction or position and is the next logical step towards building a compact, flyable system. The single-mode fiber effectively fixes the source to a single point in space, which is then collimated and fed into the system. In this way, the optical section can be interchanged among different platforms without requiring extensive re-alignment. Addition of a reference beam input through the back surface of the crystal will enable in-situ recording of the grating as well. In this scheme of operation, the ability to interchange sources to use a high power laser at the depot level for programming the correlator with new images, and utilizing a lower power, compact source on board the platform during operation, is especially useful.

CONCLUSIONS

A breadboard compact optical image correlator, using a spatial light modulator for image recording and readout, has been demonstrated. To address the issue of differing pixel dimensions, use of the same recording and readout image source (i.e. the spatial light modulator) is desired. Although Rome Laboratory's BNS SLM did not have suitable contrast at high illumination intensities, the liquid crystal display from Kopin provided a suitable performance for this task. The Kopin SLM also provides added advantages of having a standard video format and compactness in incorporating it into a next-generation optical correlator prototype. Auto- and cross-correlation results from various test images were obtained using Fourier transform images recorded using wavelength multiplexing in a LiNbO_3 crystal. This demonstrates the feasibility of implementing a compact, read-write optical correlator system as the next step.



REFERENCES

1. A.B. VanderLugt, "Signal detection by complex spatial filtering," *IEEE Trans. Inf. Theory* **IT-10**, pp. 139-146 (1964).
2. K. Sayano, G.A. Rakuljic, and G. Brost, "Application of orthogonal data storage volume holography to optical image correlation," *Proc. SPIE* **2216**, pp. 244-253 (1994).
3. K. Sayano and F. Zhao, "Narrow bandwidth, wide field of view optical filter feasibility study," Final Report, Contract No. N62269-94-C-1264 (1995).
4. K. Sayano and F. Zhao, "Storage and readout of high resolution holographic images for optical data storage and security applications," paper JTuD-10, Nonlinear Optics: Materials, Fundamentals, and Applications and ISOM/ODS, Maui, HI (1996).
5. S.A. Serati, G.D. Sharp, R.A. Serati, D.J. Knight, and J.E. Stockley, "128 x 128 analog liquid crystal spatial light modulator," *Proc. SPIE* **2490**, pp. 378-387 (1995).

MISSION OF ROME LABORATORY

Mission. The mission of Rome Laboratory is to advance the science and technologies of command, control, communications and intelligence and to transition them into systems to meet customer needs. To achieve this, Rome Lab:

- a. Conducts vigorous research, development and test programs in all applicable technologies;
- b. Transitions technology to current and future systems to improve operational capability, readiness, and supportability;
- c. Provides a full range of technical support to Air Force Material Command product centers and other Air Force organizations;
- d. Promotes transfer of technology to the private sector;
- e. Maintains leading edge technological expertise in the areas of surveillance, communications, command and control, intelligence, reliability science, electro-magnetic technology, photonics, signal processing, and computational science.

The thrust areas of technical competence include: Surveillance, Communications, Command and Control, Intelligence, Signal Processing, Computer Science and Technology, Electromagnetic Technology, Photonics and Reliability Sciences.